JOURNAL OF SOLID STATE CHEMISTRY 46, 253–264 (1983)

Phase Transitions in $CuZrF_6$ and $CrZrF_6$: A Mössbauer and EPR Study of Local and Cooperative Jahn–Teller Distortions

C. FRIEBEL, J. PEBLER, F. STEFFENS, M. WEBER, AND D. REINEN

Sonderforschungsbereich 127 and Fachbereich Chemie der Universität Marburg, Lahnberge, West Germany

Received July 1, 1982

$CuZrF_6$ and $CrZrF_6$ undergo phase transitions between 100 and 450K, which are induced by crystal packing effects and changes from dynamical to static Jahn–Teller distortions of the $Cu(Cr)F_6$ octahedra. We analyzed in particular the transitions of the Jahn–Teller type using $^{57}Fe^{2+}$, doped into the $Cu^{2+}(Cr^{2+})$ sites, as a Mössbauer probe. The quadrupole splitting is large in the region of static distortions and essentially reflects the distortion symmetry of the host $Cu(Cr)F_6$ polyhedra, while it vanishes in the case of a dynamical Jahn–Teller effect. Ligand field, EPR, and magnetic data are given in addition and are discussed with respect to the structures of the host compounds and the cooperative Jahn–Teller order of the tetragonally elongated $Cu(Cr)F_6$ polyhedra in the low-temperature phases.

1. Introduction

Transition metal compounds $T^{II}M^{IV}F_6$ frequently undergo phase transitions between the ordered cubic ReO_3(I) and the hexagonal $LiSbF_6$ structure(II) in dependence on temperature (*1*). Structural single-crystal investigations were performed, for example, with $FeZrF_6$, which crystallizes with the space groups $Fm3m$ above and $R\bar{3}$ below the transition temperature at 210K (*2, 3*), respectively. The phase transition was also studied by Mössbauer spectroscopy (*4*). The octahedrally coordinated T^{II} and M^{IV} ions are interconnected by common corners in both lattices. While the T^{II}–F–M^{IV} bonds are linear in the cubic structure (compare below, however), they are bent in the trigonal lattice. The bond angle critically depends on the size and electronic configuration of the M^{IV} ion in particular (*1*).

If T^{II} possesses an electronic E_g ground state, which is strongly σ-antibonding in an octahedral environment, as in the case of Cu^{2+} (d^9) and Cr^{2+} (d^4), strong local and cooperative Jahn–Teller distortions occur and give rise to the existence of two additional Jahn–Teller modified types of structure, which are pseudotetragonal (I′) and monoclinic (II′). The following phase transitions were found by X-ray high- and low-temperature Guinier techniques (*1*) and by neutron diffraction (*3*)—above and below the arrows, respectively—for

$$\begin{aligned} &CuZrF_6\text{: II}' \xrightarrow{353K} \text{II} \xrightarrow{383K} \text{I}, \\ &CrZrF_6\text{: II}' \xrightarrow[\approx 150K]{\approx 150K} \text{I}' \xrightarrow[415K]{393K} \text{I}, \end{aligned} \qquad (1)$$

and similarly for the corresponding Hf compounds (*1*).

The purpose of this study is to characterize the observed structures and to analyze the transitions between them with respect

0022-4596/83/020253-12$03.00/0

to the local and cooperative Jahn–Teller distortions in the dynamic and static region.

2. Experimental

The compounds $CuM^{IV}F_6$ (M^{IV} = Hf, Zr, Ti, Sn) were obtained by the dehydration of the corresponding tetrahydrates in a fluorine stream at 300–350°C for 6 hr and—in the case of Zr, Hf—the subsequent heating in sealed platinum tubes during 1 day at 800°C. The preparation of the compounds $CuM^{IV}F_6 \cdot 4H_2O$ was performed according to the method of Marignac (*5*). $CuPbF_6$ was available by heating an intimate mixture of CuF_2 and PbF_2 in F_2 at 400°C for 6 hr. The white products are extremely sensitive to moisture, yielding immediately the tetrahydrates. Only $CuPbF_6$ directly undergoes hydrolysis, yielding yellow and later brown products containing PbO_2. The anhydrous fluorides with M^{IV} = Ti, Zr, Hf crystallize in the Jahn–Teller modified $LiSbF_6$ structure type II′ at 298K (*5*). $CuPbF_6$ and $CuSnF_6$, which could not be obtained in a crystalline form, seem to possess the undeformed structure II, though the CuF_6 polyhedra are statically distorted (see below). The hydrates have a monoclinic structure, which consists of bent strings of alternating MF_6 and $Cu(OH_2)_4F_2$ polyhedra corner connected with each other via axial F^- ligands (*6*). The ligand field and EPR spectra (Figs. 1 and 2) are significantly different from those of the anhydrous compounds and will be discussed below.

A carefully dried mixture of CrF_2 and ZrF_4 (24 hr at 200°C in a stream of argon) was pressed into a tablet and heated for 50 hr at 830°C in a sealed platinum tube. The resulting product $CrZrF_6$ is greenish grey due to the presence of a small percentage of Cr^{3+} (compared below), which we could not avoid in the chosen preparation method. CrF_2 could be prepared by reacting Cr metal powder, which was cleaned with H_2 at 900°C before, with SnF_2 under argon in a closed graphite crucible according to $Cr + SnF_2 \cong CrF_2 + Sn$. The temperature was increased from 200 to 1050°C during 2 hr and the molten mixture was cooled after an additional heating period of 3 hr. The obtained greyish CrF_2 was practically free of Cr^{3+} and could be separated from Sn mechanically.

$^{57}Fe^{2+}$-doped $CrZrF_6$ was synthesized analogously to $CrZrF_6$ under addition of about 1 mole% $^{57}FeZrF_6$ to the mixture of CrF_2 and ZrF_4. The iron compound was prepared by dissolving ^{57}Fe and ZrF_4 in concentrated fluoridic acid (method of Marignac). Evaporation to dryness yielded $^{57}FeZrF_6 \cdot 6H_2O$, which was dehydrated in a stream of HF at 350°C. Similarly, $^{57}Fe^{2+}$-doped $CuZrF_6$ was obtained by the treatment of the hydrated mixed crystal—prepared according to Marignac—in a stream of dry HF. Subsequently the resulting product was heated in a sealed platinum tube for 50 hr at 800°C.

The ligand field remission spectra were recorded by a Zeiss PMQ II spectrophotometer (Infrasil) with a low-temperature attachment. We used Sr_2ZnTeO_6 (4,000–12,000 cm^{-1}) and freshly sintered MgO (8,000–30,000 cm^{-1}) as standards.

The EPR spectra were taken with a Q-band E15 Varian spectrometer with DPPH as internal standard ($g = 2.003_7$). A variable-temperature accessory (150–450 K) and low-temperature equipment (4.2K) were available.

The Mössbauer spectra were obtained with a spectrometer of the constant-acceleration type, in conjunction with a multichannel analyzer in the multiscalar mode. The room-temperature source consisted of about 20 mCi ^{57}Co diffused into metallic Rh. In the low-temperature region a variable-temperature cryostat with a Au–Fe thermocouple was used. The temperature could be kept constant within ±0.5K. The high-temperature spectra were recorded in a vacuum furnace. The temperature was

measured and controlled with an accuracy of ±1K with a chromel–alumel thermocouple. The velocity transducer was calibrated referring to the Mössbauer spectra of metallic iron. The velocity range (±7 mm · sec^{-1}) was linear within 0.3%.

In order to determine the sign of the quadrupole splitting the Mössbauer spectra of $^{57}Fe^{2+}$-doped $CrZrF_6$ were recorded in an externally applied magnetic field up to 50 kG and parallel to the γ-ray beam. The shapes of the spectra were approximately calculated by the summation over a large number of orientations of electric field gradient tensors.

3. Results and Discussion

a. Ligand Field, EPR, and Magnetic Data

The ligand field spectra (77K) of compounds $CuM^{IV}F_6$ (M^{IV} = Ti, Sn, Pb, Zr, Hf) are indicative of tetragonally distorted octahedra with an ^2E_g ground state splitting of 5850 ± 150 cm^{-1} (Fig. 1). The positions of the split states $^2B_{2g}$ and ^2E_g of the excited octahedral $^2T_{2g}$ parent level are 7800 ± 200 and 9600 ± 200 cm^{-1}, respectively, yielding an octahedral ligand field parameter Δ_0 = 6100 ± 100 cm^{-1}, fairly low compared to other copper(II)–fluoride compounds (*7*). Applying the Angular Overlap Model (*8*) the ground-state splitting 4 E_{JT} can be written as the difference of two energy parameters, describing the σ-antibonding effects in the directions of the short (e_σ^s) and the long Cu–F bond lengths (e_σ^l) in D_{4h} symmetry:

$$4\,E_{JT} = 2(e_\sigma^s - e_\sigma^l) = 2\,K_\sigma(S_\sigma^{s2} - S_\sigma^{l2}). \quad (2)$$

With tabulated overlap integrals (*9*) and a K_σ energy parameter $0.82 \cdot 10^6$ cm^{-1}, found for Cu–F bonds (*10*), long and short bond lengths of 215 and 191 pm can be estimated from Eq. (2) if the average Cu–F distance is 199 pm (*1, 11*).

The powder EPR spectrum of $CuPbF_6$ is the one expected for tetragonally elongated CuF_6 octahedra [$g_\parallel > g_\perp > g_0$ (Fig. 2)],

$$g_\parallel = g_0 + 8u_\parallel \quad \left\{u_{\parallel[\perp]} = \frac{k^2_{\parallel[\perp]}\lambda_0}{\Delta_{\parallel[\perp]}}, \qquad \text{with } \lambda_0 = 830\ cm^{-1},\right. \quad (3)$$

$$g_\perp = g_0 + 2u_\perp \quad \left.\Delta_{\parallel[\perp]} = E(^2B_{2g})\ [E(^2E_g)] - E(^2B_{1g})\right\},$$

with a nearly isotropic covalency parameter $k \simeq 0.84$, which is typical for Cu^{II}–F bonds (*7*). The g tensor of the Ti, Zr, and Hf compounds is completely different, however, with $g_\perp > g_\parallel > g_0$ and a $g_\perp$ parameter, which is distinctly split by an o-rhombic symmetry component (Table I). The g parameters are exchange narrowed (Fig. 2) and are indicative for a somewhat disturbed antiferrodistortive order of elongated octahedra (*7*), similar to the one in Fig. 3. The long Cu–F bond lengths of neighboring CuF_6 polyhedra are misaligned by $\gamma \simeq 90°$ in the (001) plane, while only short Cu–F bond distances would occur parallel to the [001] direction. For this kind of cooperative order the following coupled g tensor is expected (*7*):

$$g_\parallel^{ex} = g_\perp = g_0 + 2u_\perp,$$
$$g_\perp^{ex} = \tfrac{1}{2}(g_\parallel + g_\perp) = g_0 + 4u_\parallel + u_\perp. \quad (4)$$

With the experimental values $u_\parallel = 0.07_5$ and $u_\perp = 0.06$ one obtains $g_\parallel^{ex} = 2.12$, $g_\perp^{ex} = 2.36$ from Eq. (4)—near the observed g-parame-

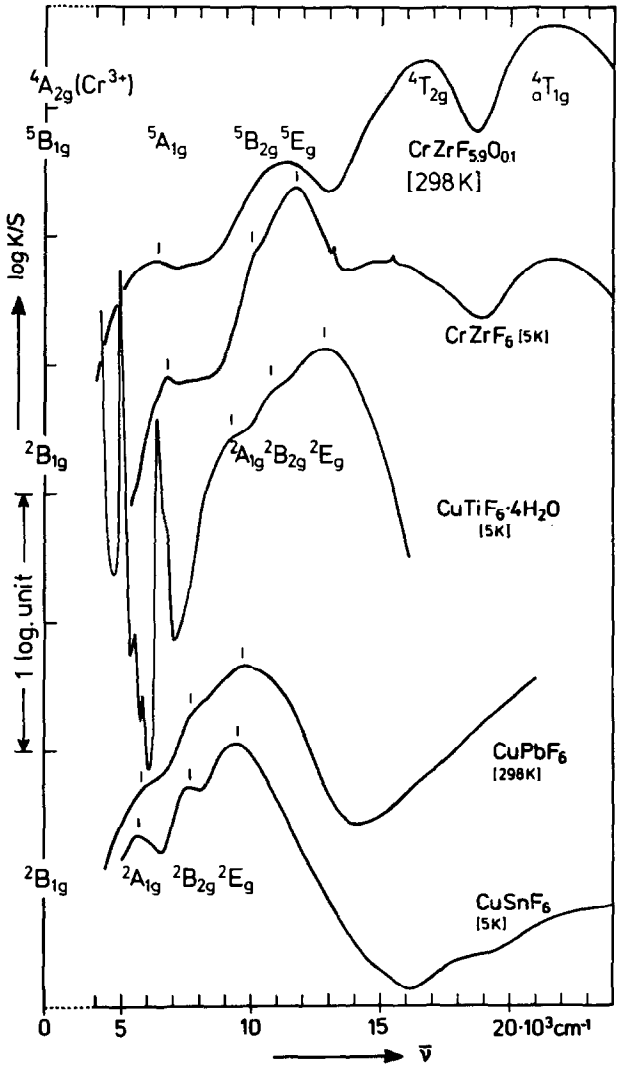

FIG. 1. Ligand field spectra of $CuM^{IV}F_6$ (M^{IV} = Sn, Pb), $CuTiF_6 \cdot 4H_2O$, and $CrZrF_6$ (assignments according to D_{4h} symmetry). The spectrum of $CrZrF_{5.9}O_{0.1}$ containing partly Cr^{3+} (assignment according to O_h symmetry) is shown in addition.

ters (Table I). In the modification II', which is the low-temperature phase of Cu(Cr)ZrF_6, the bridging F^- ligands are more displaced from the tetragonal axes (nonlinear Cu(Cr)–F–Zr bonds). The deviation of the experimental g values of $CuZrF_6$ from those calculated above for an antiferrodistortive order is due to a misalignment of the g tensor with respect to the pattern in Fig. 3 toward the threefold axis of the $LiSbF_6$-type structure. This misalignment involves in particular $g_{\parallel}^{ex}$ and the g_y^{ex} component of $g_{\perp}^{ex}$. It is also interesting to note that the increase of $g_{\parallel}^{ex}$ and the slight decrease of g_y^{ex} which is observed above 50K indicates a further movement of the g tensor toward the threefold axis.

The EPR spectrum of $CuSnF_6$ is a super-

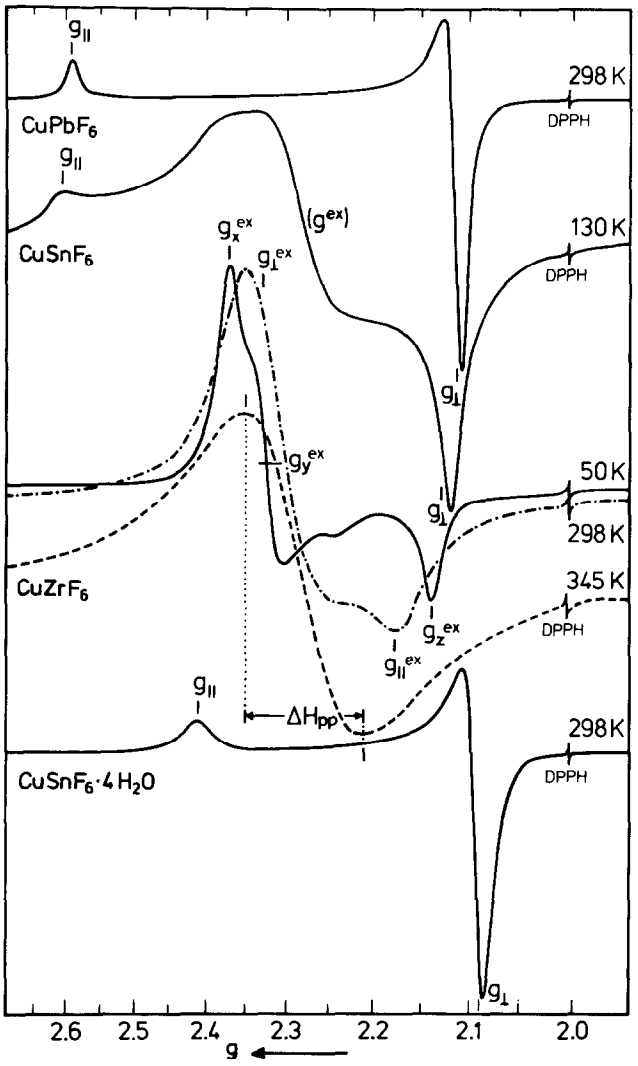

FIG. 2. EPR powder spectra (35 GHz) of compounds $CuM^{IV}F_6$ (M^{IV} = Pb, Sn, Zr) and $CuSnF_6 \cdot 4H_2O$. For further details compare text.

position of both types of spectra (with and without exchange coupling), with the uncoupled spectrum possessing about the same g values as $CuPbF_6$. A more quantitative analysis of the exchange effect and its origin will be given elsewhere (*12*).

We carefully studied the temperature dependence of the $CuZrF_6$ powder EPR spectra, in particular in the region of the phase transitions. While a resolution into anisotropic components was not possible anymore above 330K, the signal remained asymmetric until 340–345K. More detailed information is given in Fig. 4, where the variation of the linewidth (peak-to-peak distance in the anisotropic region) with temperature is shown. The lowest ΔH_{pp} value is expected, where the signal becomes isotropic. The corresponding temperature of 342 ± 5K hence describes the phase transi-

TABLE I

EPR POWDER DATA OF COMPOUNDS $CuMe^{IV}F_6$ ($g_\parallel$, $g_\perp$ LOCAL AND $g_\parallel^{ex}$, $g_\perp^{ex}$ EXCHANGE NARROWED, COOPERATIVE g PARAMETERS)

Me^{IV}	T (K)	$g_\parallel$	$g_\perp$	g_{ave}
Pb	298	2.60_5	2.11_7	2.28_0
		$g_x^{ex}(g_\perp^{ex})g_y^{ex}$	$g_\parallel^{ex}$	
Sn[a]	130		≈2.13	
	298	very broad signal	≈2.15	≈2.29
Ti	130	2.35_3 2.31_4	2.14_5	2.27_1
	298	2.33_5	2.17	2.28
Zr	≤50	2.37_0 2.32_4	2.13_4	2.27_7
	130	2.37_0 2.32_2	2.14_7	2.28_0
	260	2.36_1 2.31_8	2.17_1	2.28_3
	298	2.33_6	2.17_8	2.28_3

[a] Superimposed by a spectrum of $CuPbF_6$ type.

tion II′ ↔ II, in reasonable agreement with the X-ray value $T_u^{(1)} = 353 \pm 5$K (*1*). No further linewidth effect as an indication for the second phase transition II ↔ I, which is outside of the error limit, is found in the powder EPR spectra, however.

Magnetic susceptibility measurements of $CuZrF_6$ between 400 and 4K exhibit a linear χ^{-1} versus T dependence with a vanishing θ value. This result confirms that the exchange coupling between the CuF_6 octahedra, which is evident in the EPR spectra of, for example, $CuZrF_6$, but not of $CuPbF_6$, must be very small (*12*). The magnetic moment μ_{eff} is $2.05(5)\mu_B$, which compares rather well with the average g value obtained from the EPR spectra.

The hydrates $CuM^{IV}F_6 \cdot 4H_2O$, mentioned in the experimental section, have ligand field spectra with a considerably larger ground-state splitting ($4\,E_{JT} = 9200$ cm^{-1}) and ligand field parameter ($\Delta_0 = 7400$ cm^{-1})

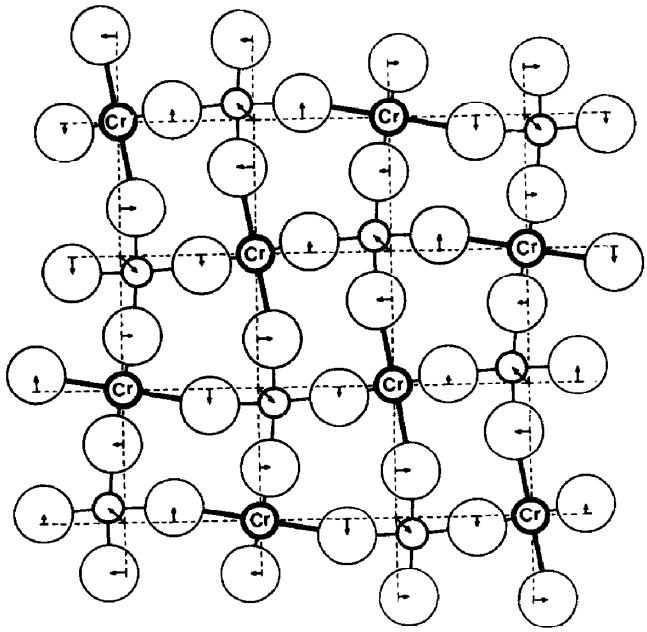

FIG. 3. The Jahn–Teller modified ordered ReO_3-type structure I′ ($CrZrF_6$ at 298K)—qualitative sketch.

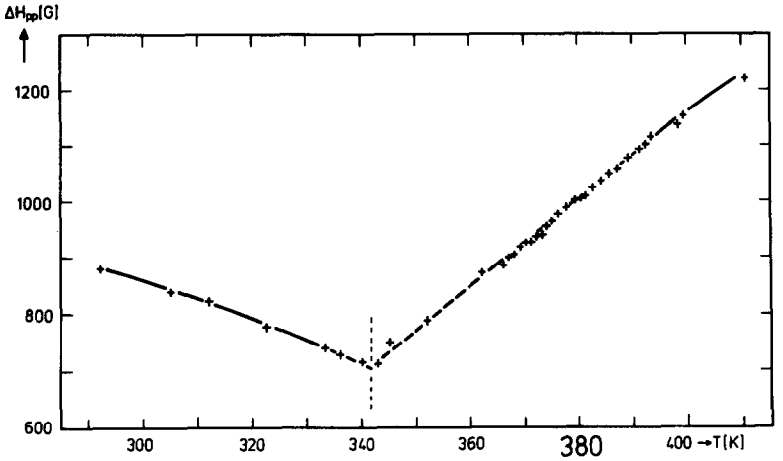

FIG. 4. Temperature dependence of the EPR linewidth for $CuZrF_6$ in the region of the II ↔ II′ phase transition (see text for details).

than the anhydrous compounds (Fig. 1). These findings agree with the very pronounced axial elongation of the CuO_4F_2 octahedra (1.96 ± 1 Å (4 × 0), 2.31 Å (2 × F)) (*6*) and the presence of four stronger equatorial OH_2 ligands instead of F^-. The split states of the octahedral $^2T_{2g}$ level are observed at 12,700 and 10,700 cm^{-1} (shoulder). The calculation of the Cu–O and Cu–F bond lengths from the ground-state splitting is again possible, utilizing the Angular Overlap Model and Eq. (2). In agreement with experimental findings (*7, 13*) an average Cu–O bond length of 2.12 Å and the same K_σ parameter of $0.82 \cdot 10^6$ cm^{-1} for the Cu–O as for the Cu–F bonds is chosen. Applying the center of gravity rule—bond length reduction in the equatorial plane of the tetragonally elongated octahedron half as large as the extension in the axial directions—and using published overlap integrals (*9*) the experimental Cu–F and Cu–O distances could be exactly reproduced. The EPR spectra are also in accord with the structural result of axially elongated octahedra in ferrodistortive order (Fig. 2). The smaller g values $g_\parallel = 2.40_7$, $g_\perp = 2.09_0$ indicate reduced orbital contributions in comparison to the anhydrous compounds, caused by the blue shift of the ligand field bands and a smaller covalency parameter $k \simeq 0.81$. k was calculated from Eq. (3); the smaller value reflects the substitution of four F^- ligands by the more covalent H_2O molecules.

The ligand field spectra of $CrZrF_6$ and $CrHfF_6$ exhibit the same features as observed for the Cu^{2+} compounds of this type (Fig. 1). The ground-state splitting is 7000 cm^{-1}, and the split-levels of the excited T_{2g} state are observed at 10,000 (shoulder) and 11,700 cm^{-1}. From these energies an octahedral Δ parameter of 7600 cm^{-1} is calculated, which is again low compared to other chromium(II)–fluoride compounds (*7*). One may suggest from the ligand field data that the CrF_6 octahedra exhibit a similar extent of distortion to the CuF_6 polyhedra. Under the assumption of an ideal antiferrodistortive order of elongated CrF_6 octahedra a distortion of about the same magnitude as in $CuZrF_6$ can also be estimated from the unit cell parameters (*1*). The Cr(II) compounds have greenish-grey colors due to the presence of a small percentage of Cr^{3+}, whose two characteristic transitions ($^4A_{2g} \rightarrow {}^4T_{2g}$, $^4T_{1g}$ at 16,800 and 22,000 cm^{-1}) can still be detected in the spectrum. The com-

parison with the mixed crystal $CrZrF_{5.9}O_{0.1}$ shows, however, that the Cr^{3+} impurity is not larger than 1–2% (Fig. 1).

The magnetic investigation yields a χ^{-1} versus T dependence with a small deviation from linearity, which indicates weak cooperative magnetic interactions at low temperatures. The magnetic moments are $4.9\mu_B$ above 200K, very near to the spin-only value for a high-spin d^4 configuration—as expected in a strongly tetragonal ligand field.

b. Mössbauer Spectroscopy

The isomeric shift of $CuZrF_6$ and $CrZrF_6$, doped by about 1 mole% $^{57}Fe^{2+}$ in the transition metal position, relative to metallic iron (298K) was δ = 1.462(8) and 1.463(8) mm sec^{-1}, respectively. The corresponding shift for $FeZrF_6$ is 1.427(8) mm sec^{-1} (*4*); all

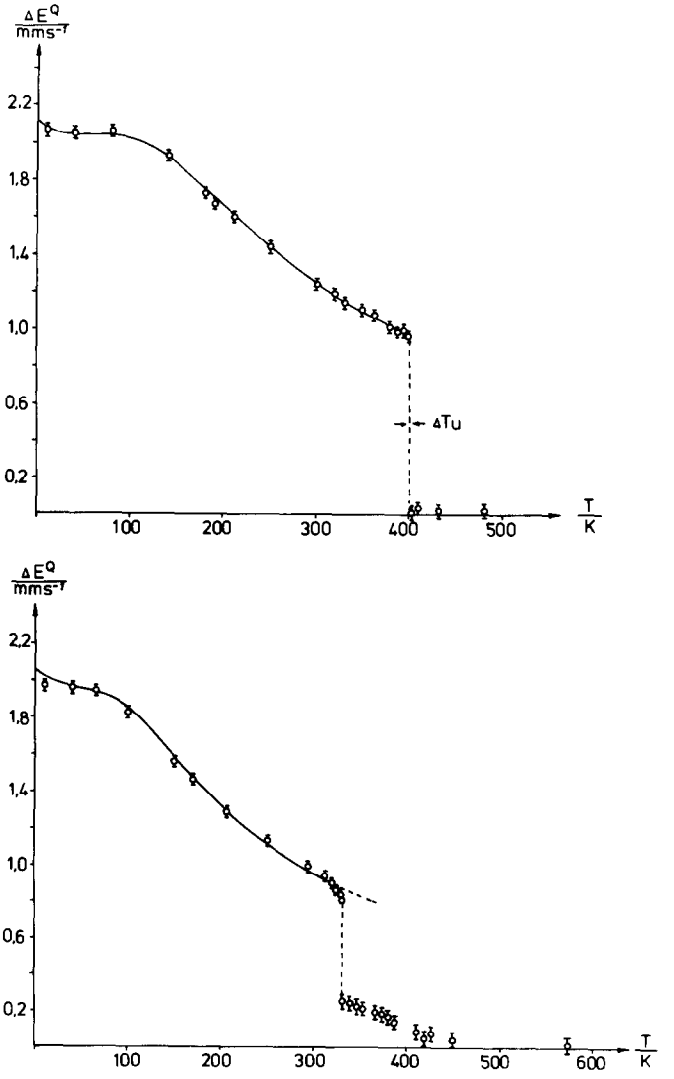

FIG. 5. Temperature dependence of the quadrupole splitting ΔE^Q for $^{57}Fe^{2+}$-doped $CrZrF_6$ (above) and $CuZrF_6$ (below).

these values are indicative for high-spin Fe^{2+} ions in ionic bonding.

Applying a magnetic field of $H = 50$ kG parallel to the γ-ray beam the two-line zero-field spectrum of $^{57}Fe^{2+}$-doped $CrZrF_6$ at $T = 4.2$K splits into a doublet and a triplet, where the doublet is due to the $\langle \pm\frac{1}{2}| \rightarrow \langle \pm\frac{3}{2}|$ transitions. Because the triplet appears at a higher velocity than the doublet, the sign of the quadrupole splitting and hence the field gradient q is negative.

The large quadrupole splitting ΔE^Q in dependence on temperature (Fig. 5) is taken as evidence that the Fe^{2+} ions reflect the considerable local distortions of the CuF_6 and CrF_6 polyhedra in the different phases (*14*). The curves below 400 ($CrZrF_6$) and 330K ($CuZrF_6$) can be reproduced on the basis of splitting parameters Δ_1 and Δ_2, which are defined in Fig. 6 as due to a tetragonal distortion, either with D_{4h} symmetry (Δ_2; $\Delta_1 = 0$) or with an additional o-rhombic (Δ_2, Δ_1) component. Explicitly, the procedure of Ingalls (*15*) is used:

$$\Delta E^Q(T) = \tfrac{2}{7}e^2Q(1 - R_0)\overline{r^{-3}} \frac{\alpha^2\lambda}{\lambda_0} F(\Delta_i, \alpha^2\lambda, T). \quad (5)$$

Equation (5) accounts for partial covalent bonding by the reduction factor α. The parameter F is a function of the thermal occupation of the split levels, which originate from the $^5T_{2g}$ ground state by spin–orbit coupling ($\alpha^2\lambda$; $\lambda_0 = 103$ cm^{-1}) and the ligand field influence (Δ_1, Δ_2). This model was also applied to $FeZrF_6$ and is explained in more detail elsewhere (*4*).

The phase transition II′ ↔ I′ for $CrZrF_6$ is not seen by Mössbauer spectroscopy. This is in accord with the structural and ligand field spectroscopic evidence that statically distorted CrF_6 polyhedra are present in both phases, which are only distinguished by different Cr–F–Zr bridging angles. On the other hand, the transition from a static to a dynamic local Jahn–Teller distortion (I ↔ I′) is clearly visible, with a vanishing quadrupole splitting in the cubic phase. Obviously the reorientation time τ_R, which is connected with the dynamic change of the tetragonal axis between the three fourfold axes of the FeF_6 octahedron (pseudorotation around a threefold axis), is small with respect to the observation time of the Mössbauer experiment ($\tau_R = \hbar/\Delta E^Q \simeq 10^{-8}$ sec). The phase transition is of first order. A two-phase region of $\Delta T_u^{(2)} \simeq 6.5$K is observed—not unexpected in a powder experiment with a rather large particle size distribution (Figs. 5 and 7). The transition temperature $T_u^{(2)} = 400 \pm 5$K is slightly

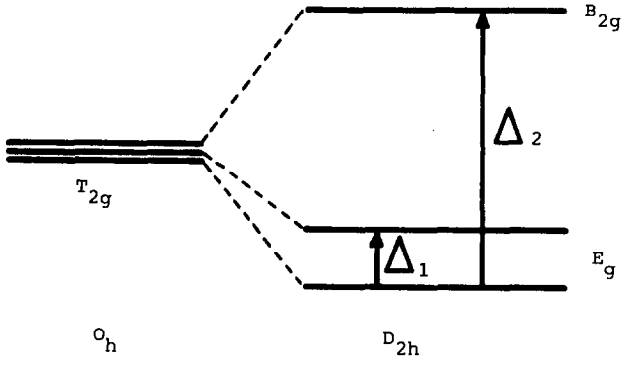

FIG. 6. Splitting of the octahedral $^5T_{2g}$ ground state for Fe^{2+} by a tetragonal distortion (axial elongation), with an o-rhombic symmetry component superimposed ($\Delta_1 \neq 0$) (without LS coupling; term designation in D_{4h}).

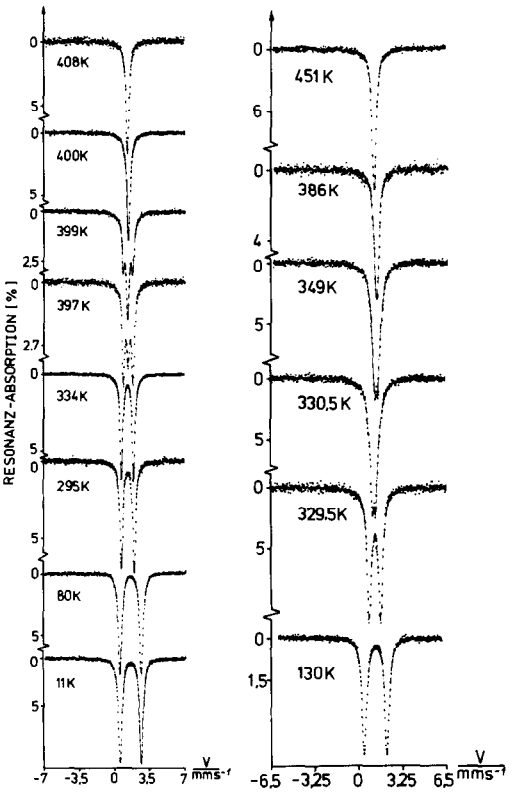

FIG. 7. Mössbauer spectra of $^{57}Fe^{2+}$ ions doped into the transition metal positions of $CrZrF_6$ (left) and $CuZrF_6$ (right).

higher than that found by X-ray and somewhat lower than that found by neutron diffraction (Eq. (1)). Both methods are less sensitive than the quadrupole splitting, however. The sign of the field gradient q, as obtained from the magnetic field experiment, gives evidence for tetragonally elongated FeF_6 octahedra (*14*), which obviously reflect the distortion geometry of the CrF_6 entities. From the temperature dependence of ΔE^Q below 400K the following parameters are explicitly obtained:

$$\alpha^2\lambda = -65\ \text{cm}^{-1}; \qquad \Delta_1 = 75(5)\ \text{cm}^{-1}; \qquad \Delta_2 = 247(10)\ \text{cm}^{-1}. \quad (6)$$

The presence of an additional orthorhombic symmetry component is in agreement with the predictions from the Jahn-Teller theorem for an octahedral d^6 configuration. It splits the orbital doublet (D_{4h}, elongation) and leads to an orbitally nondegenerate ground state (Fig. 6).

In the case of $^{57}Fe^{2+}$-doped $CuZrF_6$ a first-order phase transition II′ → II, which is connected with the change from statically to dynamically distorted FeF_6 octahedra, is observed at $T_u^{(1)} = 330 \pm 5$K (Fig. 5), somewhat lower than that found for the pure compound $CuZrF_6$ by X-ray techniques and EPR spectroscopy (see above). The quadrupole splitting remains finite in the $LiSbF_6$ lattice II, however. This finding is expected, because the octahedra of this structure are slightly compressed along a threefold axis (*1*), in agreement with the temperature dependence of ΔE^Q for $FeZrF_6$ (*4*). While this symmetry argument readily accounts for the remaining quadrupole splitting between $T_u^{(1)}$ and $T_u^{(2)}$ (= 383 ± 5K), it is somewhat surprising that ΔE^Q is still nonvanishing even above $T_u^{(2)}$, though the splitting is very small (Figs. 5 and 7). The reason is possibly that in cubic $CuZrF_6$ with space group $Fm3m$ there are *statistical* deviations of the F^- positions from the Cu–Zr directions of the same kind as occur in the $LiSbF_6$ structure with space group $R\bar{3}$ in an *ordered* manner. These deviations are expected to impose a tiny trigonal distortion on the octahedra. This argument also gives the most obvious explanation for the anomalous behavior, which the cubic unit cell parameter a shows in dependence on temperature above $T_u^{(2)}$ (*11*). While a increases with a gradient of $1.8 \cdot 10^{-4}$ Å/K between 383 and 458K, the increase $\Delta a/\Delta T$ is only $1.4 \cdot 10^{-5}$ Å/K above 458K. In the former temperature interval the F^- ligands seem to move toward positions, which imply linear Cu–F–Zr bonds with undistorted octahedra. The final position is reached at 458K, and—consistent with this model—at about the same temperature the quadrupole splitting becomes zero. In cubic $FeZrF_6$ no anomalies in the a versus T dependence are

observed, in accord with $\Delta E^Q = 0$ above the II ↔ I phase transition (*4*). The possible deviations of F^- from linear T^{II}–F–M^{IV} bonds in a cubic space group are further considered in a neutron diffraction study of compounds $T^{II}M^{IV}F_6$ (*3*). From the temperature dependence of the quadrupole splitting below $T_u^{(1)} = 330$K ligand field parameters very similar to those of $CrZrF_6$ ($^{57}Fe^{2+}$) are calculated:

$$\alpha^2\lambda = -65 \text{ cm}^{-1}; \quad \Delta_1 = 90(5) \text{ cm}^{-1}; \quad \Delta_2 = 230(10) \text{ cm}^{-1}. \quad (7)$$

The Mössbauer linewidth for the statically distorted FeF_6 octahedra is $\Gamma = 0.31$ mm sec^{-1}, while it is slightly larger (0.35 mm sec^{-1}) in the dynamic region. The temperature influence on the linewidth and lineshape has not been considered yet.

Figure 8 shows a 5K Mössbauer spectrum of $CuZrF_6$, which was briefly exposed to air and hence partly transformed to the tetrahydrate. It is immediately obvious by comparison with the other spectra that the doublet component with the larger quadrupole splitting is due to $CuZrF_6 \cdot 4H_2O$—consistent with the ligand field and EPR data discussed before.

It seems worthwhile to translate the splitting parameters Δ_2 (and Δ_1), which were deduced from the experiment for the FeF_6 polyhedra in Cr(Cu)ZrF_6 (Eqs. (6) and (7)), into Fe–F bond lengths, utilizing suitable theoretical models. We have already successfully done this for trigonal distortions of the FeF_6 octahedra in $FeZrF_6$ (*4*). In the crystal field model the splitting of the $^5T_{2g}$ ground state by a tetragonal component

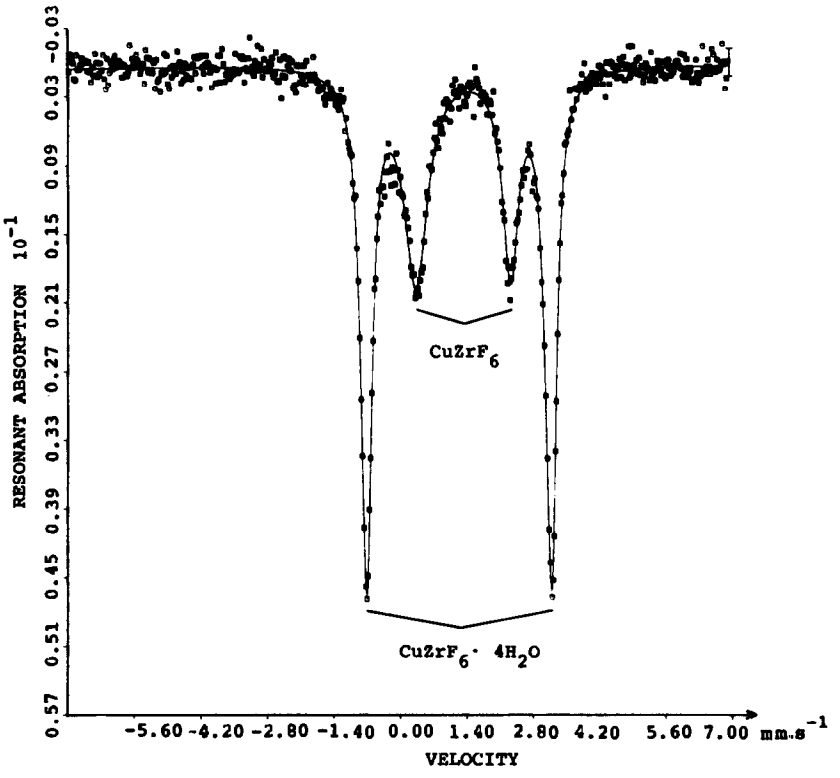

FIG. 8. Mössbauer spectrum (10K) of $CuZrF_6$ ($^{57}Fe^{2+}$) ($\Delta E^Q = 2.00$ mm sec^{-1}), partly transformed into $CuZrF_6 \cdot 4H_2O$ ($^{57}Fe^{2+}$) ($\Delta E^Q = 3.90$ mm sec^{-1}).

(elongation) (*14*) is $\Delta_2^1 = 3\,Ds - 5\,Dt$ (Fig. 6), where

$$Ds = -\frac{2}{7}\frac{e^2}{R_0^3}\overline{r^2}\left\{\frac{1}{(1+2\delta')^3} - \frac{1}{(1-\delta')^3}\right\} \simeq \frac{18}{7}\delta'\frac{e^2}{R_0^3}\overline{r^2}, \quad (6)$$

$$Dt = -\frac{2}{21}\frac{e^2}{R_0^5}\overline{r^4}\left\{\frac{1}{(1+2\delta')^5} - \frac{1}{(1-\delta')^5}\right\} \simeq \frac{10}{7}\delta'\frac{e^2}{R_0^5}\overline{r^4}.$$

$R_0 + 2\delta$ (2×) and $R_0 - \delta$ (4×) are the bond lengths in a tetragonally elongated FeF_6 polyhedron ($\delta' = \delta/R_0$). Though the octahedral ionic radii of Cu^{2+} (0.73 Å) and Cr^{2+} (0.82 Å) deviate somewhat from that of Fe^{2+} (0.77 Å), we choose as Fe–F bond distance R_0 that in $FeZrF_6$ (2.05 Å (2)). The calculated radial integrals for the free Fe^{2+} ion are $\overline{r^2} = 0.3901$, $\overline{r^4} = 0.3525$ Å (*16, 4*). With these numbers and Δ_2^1 energies of 285 ($CrZrF_6$) and 275 cm^{-1} ($CuZrF_6$) (neglecting the o-rhombic symmetry component; Eqs. (5) and (6) and Fig. 6) a δ value of 0.017 Å is calculated. Even if one considers the rather crude model, the static distortion of the FeF_6 octahedron (a(Fe–F) $\simeq 2.08_5$ Å (2×); 2.03_5 Å (4×)) is certainly smaller than that of the Cu^{2+} or Cr^{2+} host sites.

After all Mössbauer spectroscopy turns out to be a sensitive tool for analyzing structural phase transitions of the Jahn–Teller type—in particular with respect to local distortions of the static and dynamic type.

References

1. D. Reinen and F. 'Steffens, *Z. Anorg. Allg. Chem.* **441,** 63 (1978).
2. P. Köhl, D. Reinen, G. Decher, and B. Wanklyn, *Z. Kristallogr.* **153,** 211 (1980).
3. H. W. Mayer, D. Reinen, and G. Heger, *J. Solid State Chem.*, to be published.
4. J. Pebler, K. Schmidt, F. Steffens, and D. Reinen, *J. Solid State Chem.* **25,** 107 (1978).
5. F. Steffens and D. Reinen, *Z. Naturforsch. B* **31,** 894 (1976).
6. J. Fischer, A. de Cian, and R. Weiss, *Bull. Soc. Chim.* **8,** 2646 (1966).
7. D. Reinen and C. Friebel, "Structure and Bonding," Vol. 37, pp. 1–60, Springer-Verlag, Berlin (1979).
8. C. K. Jørgensen, *in* "Modern Aspects of Ligand Field Theory," North-Holland, Amsterdam (1970).
9. D. W. Smith, "Structure and Bonding," Vol. 12, pp. 87–118, Springer-Verlag, Berlin (1972).
10. D. Reinen and S. Krause, *Inorg. Chem.* **20,** 2750 (1981).
11. V. Propach and F. Steffens, *Z. Naturforsch. B* **33,** 268 (1978).
12. C. Friebel, S. Kremer, and D. Reinen, to be published.
13. D. Reinen and H. Weitzel, *Z. Anorg. Allg. Chem.* **31,** 424 (1976).
14. The possibility that the quadrupole splitting is induced by a distortion along an octahedral threefold axis (elongation) is not considered, because the isomorphous substitution of Cu^{2+} or Cr^{2+} by Fe^{2+} will most probably impose a predominantly tetragonal symmetry on the FeF_6 polyhedra also.
15. R. Ingalls, *Phys. Rev. A* **133,** 787 (1964).
16. A. Abragam and B. Bleaney, *in* "Electron Paramagnetic Resonance of Transition Ions," Oxford Univ. Press (Clarendon), Oxford (1970).